INTERNATIONAL JOURNAL FOR NUMERICAL METHODS IN FLUIDS, VOL. 10, 683–695 (1990)

A COMPUTATIONAL METHOD FOR SIMULATING TRANSIENT MOTIONS OF AN INCOMPRESSIBLE INVISCID FLUID WITH A FREE SURFACE

TSUKASA NAKAYAMA

Department of Precision Mechanical Engineering, Faculty of Science and Engineering, Chuo University, 13-27, Kasuga 1-chome, Bunkyo-ku Tokyo 112, Japan

SUMMARY

A new numerical method has been developed for the analysis of unsteady free surface flow problems. The problem under consideration is formulated mathematically as a two-dimensional non-linear initial boundary value problem with unknown quantities of a velocity potential and a free surface profile. The basic equations are discretized spacewise with a boundary element method and timewise with a truncated forward-time Taylor series. The key feature of the present paper lies in the method used to compute the time derivatives of the unknown quantities in the Taylor series.

The use of the Taylor series expansion has enabled us to employ a variable time-stepping method. The size of time increment is determined at each time step so that the remainders of the truncated Taylor series should be equal to a given small error limit. Such a variable time-stepping technique has made a great contribution to numerically stable computations.

A wave-making problem in a two-dimensional rectangular water tank has been analysed. The computational accuracy has been verified by comparing the present numerical results with available experimental data. Good agreement is obtained.

KEY WORDS Free surface flow Boundary element method Taylor series expansion Water waves

INTRODUCTION

The continuing development of high-speed digital computers has encouraged and enabled us to analyze numerically complicated flow phenomena of fluids. This is particularly true of free surface flow problems. Unsteady motions of a fluid with free surfaces are formulated mathematically as non-linear initial boundary value problems. Numerical and analytical solutions of the problem have been difficult to achieve for two main reasons: (1) the position of the free surface varies with time in a manner not known *a priori* and must be found as a part of the solutions; (2) the boundary conditions on the free surface are non-linear equations.

When assuming a fluid to be incompressible and inviscid and a flow to be irrotational, the fluid flow is governed by the Laplace equation expressed in terms of a velocity potential. It is well known that the solution of the Laplace equation is expressed in terms of boundary integrals of a harmonic function and its normal derivative. Using this form of solution, a two-dimensional flow problem, for example, is transformed into a one-dimensional problem governed by a boundary integral equation of the Fredholm type, and the dimension of the problem can be reduced by one. This is a great advantage in reducing computer memory and computing time requirements.

0271–2091/90/060683–13$06.50

Received 17 October 1988
Revised 10 July 1989

Such a solution technique, called a boundary element method, has been successfully applied to a number of two-dimensional free surface flow problems, including overturning of water waves,[1,2] liquid sloshing in tanks subjected to forced oscillations[3,4] and wave-making problems.[5,6] Although the methods proposed so far are well designed and are powerful tools for some kinds of free surface flows, most of them are poor in numerical stability for large distortions or rapid movements of free surfaces.

In 1984, Dold and Peregrine[7] proposed a simple and cost-effective method based on the complex variable boundary element method. They used forward-time Taylor series expansions in a time-stepping procedure and realized stable computations in the analysis of wave-breaking phenomena. Their numerical method, however, has been specialized under some assumptions for the purpose of the numerical simulation of breaking waves. Furthermore, the use of complex variables restricts the method to two-dimensional problems.

In this paper the original method of Dold *et al.* has been extended and modified. The present method can be applied to the analysis of various types of free surface flow problems in water tanks. Although our final goal is to construct a numerical method for three-dimensional free surface flows, the focus of the present paper is on two-dimensional flows in order to verify the applicability of the proposed method.

MATHEMATICAL DESCRIPTION OF A FREE SURFACE FLOW PROBLEM

To show the detail of the proposed method, we construct here an example of an unsteady free surface flow problem.

Consider a wave generation problem[8] in the two-dimensional water tank shown in Figure 1. The tank has a width $2W$ and is filled with water to a constant height h in the stationary condition. A wave generator of the piston type with a width $2b$ is set at the centre of the tank bottom and is permitted to move upwards according to the displacement function

$$Y_P(t) = Y_0[1 - \exp(-\alpha t)] \quad \text{for } t > 0. \tag{1}$$

A rectangular Cartesian co-ordinate system o-xy is fixed to the tank in such a manner that the x-axis coincides with the stationary free surface and the y-axis coincides with the centreline of the tank. Since the fluid motion caused by the wave generator will be symmetric, the fluid region $x \geqslant 0$ is chosen as the solution domain. The fluid is assumed to be inviscid and incompressible,

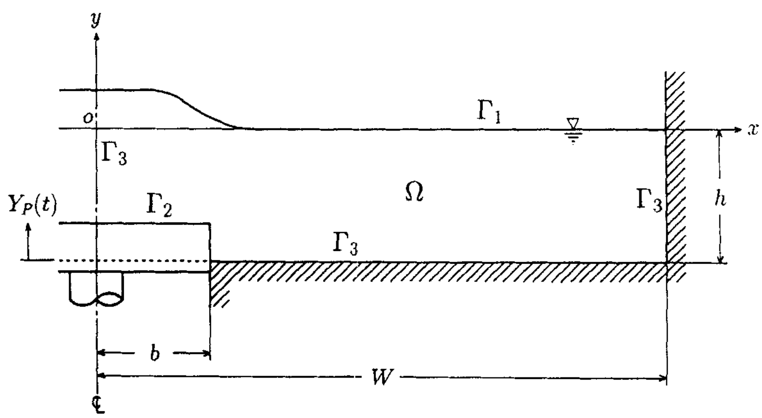

Figure 1. A two-dimensional water tank with a wave generator

and the flow to be irrotational. These assumptions permit us to introduce the velocity potential $\phi(x, y, t)$ defined by

$$\frac{\partial \phi}{\partial x} = u, \qquad \frac{\partial \phi}{\partial y} = v. \tag{2}$$

Here u and v are the x- and y-components of the fluid velocity respectively. Then the governing equation to be solved is given by

$$\nabla^2 \phi = 0 \quad \text{in } \Omega, \tag{3}$$

where Ω denotes the solution domain. The boundary conditions are as follows:[6]

$$\frac{\mathrm{D}\phi}{\mathrm{D}t} - \tfrac{1}{2}(u^2 + v^2) + g\eta = 0 \quad \text{on } \Gamma_1, \tag{4}$$

$$u = \frac{\mathrm{D}\xi}{\mathrm{D}t}, \qquad v = \frac{\mathrm{D}\eta}{\mathrm{D}t} \quad \text{on } \Gamma_1, \tag{5}$$

$$\frac{\partial \phi}{\partial n} = -\frac{\mathrm{d}Y_{\mathrm{P}}}{\mathrm{d}t} \quad \text{on } \Gamma_2, \tag{6}$$

$$\frac{\partial \phi}{\partial n} = 0 \qquad \text{on } \Gamma_3, \tag{7}$$

where Γ_1, Γ_2 and Γ_3 represent the free surface, the upper surface of the piston and the remaining part of the boundary respectively, $\mathrm{D}/\mathrm{D}t$ denotes Lagrangian time differentiation, $\partial/\partial n$ denotes differentiation in the direction of the outward normal n on the boundary, g is the acceleration due to gravity and (ξ, η) are the co-ordinates of fluid particles on the free surface. In the present method a finite number of particles distributed along the free surface are moved every time step in a Lagrangian manner to simulate the change of the free surface profile. Condition (5) expresses the property that a fluid particle remains on the free surface during subsequent fluid motions once it lies on the free surface. The unknown quantities of the problem are ξ, η and ϕ.

When calculations are started from a stationary condition of the fluid, the initial conditions are given as follows:

$$\left.\begin{array}{l} \phi = \eta = 0 \\ \xi \text{ specified} \end{array}\right\} \quad \text{at } t = 0. \tag{8}$$

SOLUTION PROCEDURE

Consider two successive time instants t and $t + \Delta t$ and suppose that a fluid particle on the free surface moves from the position (ξ, η) to the position (ξ', η') during the time interval Δt as shown in Figure 2. The kinematic condition (5) ensures that the new position (ξ', η') also lies on the free surface. Then ξ' and η' are expanded into Taylor series about (ξ, η, t) and truncated at the term of nth-order derivatives as

$$\xi' \approx \xi + \Delta t \frac{\mathrm{D}\xi}{\mathrm{D}t} + \frac{(\Delta t)^2}{2!}\frac{\mathrm{D}^2\xi}{\mathrm{D}t^2} + \frac{(\Delta t)^3}{3!}\frac{\mathrm{D}^3\xi}{\mathrm{D}t^3} + \dots + \frac{(\Delta t)^n}{n!}\frac{\mathrm{D}^n\xi}{\mathrm{D}t^n}, \tag{9}$$

$$\eta' \approx \eta + \Delta t \frac{\mathrm{D}\eta}{\mathrm{D}t} + \frac{(\Delta t)^2}{2!}\frac{\mathrm{D}^2\eta}{\mathrm{D}t^2} + \frac{(\Delta t)^3}{3!}\frac{\mathrm{D}^3\eta}{\mathrm{D}t^3} + \dots + \frac{(\Delta t)^n}{n!}\frac{\mathrm{D}^n\eta}{\mathrm{D}t^n}. \tag{10}$$

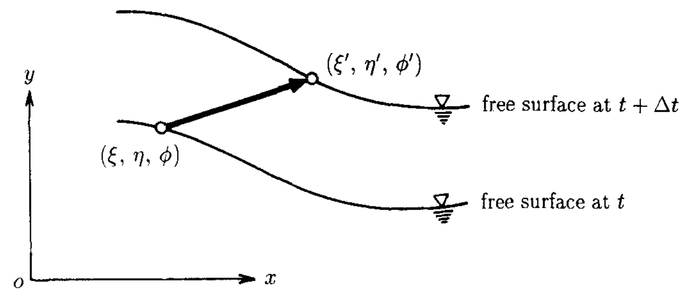

Figure 2. Movement of a fluid particle on the free surface

Let ϕ and ϕ' denote the values of the velocity potential at (ξ, η) and (ξ', η') respectively. Then, similarly, ϕ' can be approximated as follows:

$$\phi' \approx \phi + \Delta t \frac{\mathrm{D}\phi}{\mathrm{D}t} + \frac{(\Delta t)^2}{2!}\frac{\mathrm{D}^2\phi}{\mathrm{D}t^2} + \frac{(\Delta t)^3}{3!}\frac{\mathrm{D}^3\phi}{\mathrm{D}t^3} + \dots + \frac{(\Delta t)^n}{n!}\frac{\mathrm{D}^n\phi}{\mathrm{D}t^n}. \tag{11}$$

If each term of these Taylor series is evaluated, the new position of the free surface and the new value of the velocity potential on the free surface can be found. Now our attention is focused on the way to evaluate Lagrangian time derivatives of ξ, η and ϕ at time t.

First-order Lagrangian derivatives

In the first stage of the computation we solve the boundary value problem

$$\nabla^2\phi = 0 \qquad \text{in } \Omega, \tag{12}$$

$$\phi = \hat{\phi} \qquad \text{on } \Gamma_1, \tag{13}$$

$$\frac{\partial\phi}{\partial n} = -\frac{\mathrm{d}Y_{\mathrm{P}}}{\mathrm{d}t} \qquad \text{on } \Gamma_2, \tag{14}$$

$$\frac{\partial\phi}{\partial n} = 0 \qquad \text{on } \Gamma_3, \tag{15}$$

where the specified potential value $\hat{\phi}$ is computed at the previous time step. The boundary element method is used to solve the problem and equations (12)–(15) are transformed into the following boundary integral equation via Green's second identity:

$$\alpha_{\mathrm{P}}\phi_{\mathrm{P}} - \int_{\Gamma_1} \frac{\partial\phi}{\partial n} \ln\frac{1}{r}\,\mathrm{d}\Gamma + \int_{\Gamma_2+\Gamma_3} \phi\frac{\partial}{\partial n}\left(\ln\frac{1}{r}\right)\mathrm{d}\Gamma = -\int_{\Gamma_2} \frac{\mathrm{d}Y_{\mathrm{P}}}{\mathrm{d}t}\ln\frac{1}{r}\,\mathrm{d}\Gamma - \int_{\Gamma_1} \hat{\phi}\frac{\partial}{\partial n}\left(\ln\frac{1}{r}\right)\mathrm{d}\Gamma, \tag{16}$$

where r is the distance between a source point P on the boundary and an observation point Q which also lies on the boundary. If P is on a smooth part of the boundary the coefficient α_{P} takes the value π, and it is the interior angle between two tangents at P if P lies on a corner point. ϕ_{P} denotes the value of the velocity potential at P. The solution of the integral equation (16) yields $\partial\phi/\partial n$ on the free surface. Since the potential values are already known along the free surface, the tangential derivative $\partial\phi/\partial s$ can be calculated by numerical differentiation. (The formulae for the numerical differentiation and their derivation are described in the Appendix.) Then $\mathrm{D}\xi/\mathrm{D}t$ and

$D\eta/Dt$ are evaluated by

$$\frac{D\xi}{Dt} = u = \frac{\partial\phi}{\partial x} = \frac{\partial\phi}{\partial n} l - \frac{\partial\phi}{\partial s} m, \tag{17}$$

$$\frac{D\eta}{Dt} = v = \frac{\partial\phi}{\partial y} = \frac{\partial\phi}{\partial n} m + \frac{\partial\phi}{\partial s} l, \tag{18}$$

where l and m are the x- and y-components of the unit normal vector drawn outwardly on the free surface. $D\phi/Dt$ is calculated using the dynamic condition (4) as

$$\frac{D\phi}{Dt} = \tfrac{1}{2}(u^2 + v^2) - g\eta. \tag{19}$$

Second-order Lagrangian derivatives

The second-order Lagrangian derivative $D^2\xi/Dt^2$, for example, is expressed as

$$\frac{D^2\xi}{Dt^2} = \frac{Du}{Dt} = \frac{\partial u}{\partial t} + u\frac{\partial u}{\partial x} + v\frac{\partial u}{\partial y} = \frac{\partial\phi_t}{\partial x} + u\frac{\partial u}{\partial x} + v\frac{\partial u}{\partial y}, \tag{20}$$

where $\phi_t = \partial\phi/\partial t$. To evaluate $D^2\xi/Dt^2$ we must know the first-order Eulerian time derivative ϕ_t of the velocity potential.

By differentiating the Laplace equation (3) with respect to time, it can be easily found that ϕ_t satisfies the Laplace equation as ϕ does. Then we solve the following boundary value problem:

$$\nabla^2\phi_t = 0 \quad \text{in } \Omega, \tag{21}$$

$$\phi_t = \frac{D\phi}{Dt} - (u^2 + v^2) \quad \text{on } \Gamma_1, \tag{22}$$

$$\frac{\partial\phi_t}{\partial n} = -\left(\frac{d^2 Y_P}{dt^2} + \frac{dY_P}{dt}\frac{\partial u}{\partial x}\right) \quad \text{on } \Gamma_2, \tag{23}$$

$$\frac{\partial\phi_t}{\partial n} = 0 \quad \text{on } \Gamma_3. \tag{24}$$

It should be noted that the right-hand side of equation (22) is already known and that condition (22) gives Dirichlet data. The boundary condition (23) is derived by differentiating equation (6) with respect to time. Since the boundary Γ_2 is the moving one with velocity dY_P/dt, the Lagrangian differentiation should be done using the differential operator defined by

$$\frac{\partial}{\partial t} + \left(\frac{dY_P}{dt}\right)\frac{\partial}{\partial y}.$$

The boundary element solution for this problem gives $\partial\phi_t/\partial n$ on the free surface. The tangential derivative $\partial\phi_t/\partial s$ is computed by numerical differentiation. These spatial derivatives are then transformed as

$$\frac{\partial\phi_t}{\partial x} = \frac{\partial\phi_t}{\partial n} l - \frac{\partial\phi_t}{\partial s} m, \tag{25}$$

$$\frac{\partial\phi_t}{\partial y} = \frac{\partial\phi_t}{\partial n} m + \frac{\partial\phi_t}{\partial s} l. \tag{26}$$

On the other hand, the spatial derivatives of the velocity components are calculated by numerical differentiation as shown in the Appendix. Thus $D^2\xi/Dt^2$ is evaluated with expression (20). $D^2\eta/Dt^2$ is also calculated in the same way.

The second-order Lagrangian derivative of ϕ is evaluated with

$$\frac{D^2\phi}{Dt^2} = u\frac{Du}{Dt} + v\frac{Dv}{Dt} - gv, \tag{27}$$

which is given by differentiating the dynamic boundary condition (4) with respect to time.

Higher-order Lagrangian derivatives

We proceed in the same way to calculate higher-order Lagrangian derivatives of ξ, η and ϕ up to the order of n. In the present formulation n is taken as $n = 3$.

BOUNDARY ELEMENT METHOD

As mentioned in the previous section, the boundary value problems of ϕ and its Eulerian time derivatives are solved by the boundary element method. The boundary element formulation starts from the derivation of integral equations of the type of equation (16).

The boundary of the solution domain is divided into a large number of line elements. In each element, Φ and $\partial\Phi/\partial n$ (Φ is ϕ, ϕ_t or a higher-order Eulerian time derivative of ϕ) are approximated by linear shape functions. Thus the integral equation is reduced to a set of linear algebraic equations with the unknown variables $\partial\Phi/\partial n$ on the free surface and Φ on the remaining part of the boundary.

We mention here the treatment of nodal points at the intersections of Γ_1 and Γ_3. These intersections are the so-called corner points where the value of $\partial\Phi/\partial n$ is discontinuous and two values of $\partial\Phi/\partial$n exist. Then, in the present boundary element formulation, double nodes are laid at the corner point as shown in Figure 3, where node A belongs to the free surface and node B belongs to the solid wall. At node A, $\partial\Phi/\partial n_1$ is assigned and is treated as an unknown quantity, while $\partial\Phi/\partial n_2$ is assigned at node B and is known to vanish from the boundary condition (7). On the other hand, Φ itself should be continuous at that intersection. Therefore a subsidiary condition

$$\Phi_A = \Phi_B$$

must be considered when the boundary integral equations are solved.

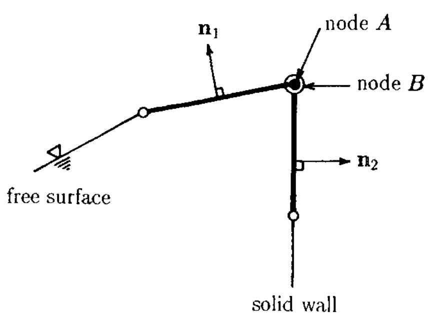

Figure 3. Overlapped nodes at a corner point

A set of linear algebraic equations thus derived is solved by the LU decomposition method. In order to determine the values of Φ, several sets of equations are to be solved per time step. However, since they are assembled at the same time instant and for the same free surface profile, they have the same coefficient matrix. Therefore, once the coefficient matrix is decomposed into a lower and an upper triangular matrix, we have only to do the forward and backward substitutions for individual solutions of the equations.

It is emphasized that the present boundary element formulation is different from that of Dold *et al.*[7] Their method is constructed for the special purpose of the numerical simulation of wave-breaking phenomena. By assuming the periodicity of water waves and using the principle of reflection, they eliminated unknown variables on the parts of the boundary except the free surface when formulating the problem mathematically. Their derived integral equation consists only of the boundary integral along the free surface. The resulting system of linear algebraic equations is easy to solve by iterative methods, and less computing time may be required than in LU decomposition or matrix inversion. The applicable field of their method is, however, greatly restricted. Furthermore, the complex variable boundary element method used by them cannot be extended to three-dimensional versions. This is the main reason why the boundary element method based on Green's identity has been adopted in the present method.

VARIABLE TIME-STEPPING TECHNIQUE

The size of the time increment is calculated every time step by controlling the remainder of truncated Taylor series.[9] A Taylor expansion of a function $f(t)$ is expressed as

$$f(t+\Delta t) = f(t) + \Delta t f'(t) + \frac{(\Delta t)^2}{2!} f''(t) + \frac{(\Delta t)^3}{3!} f'''(t) + \dots . \tag{28}$$

When this Taylor series is truncated as

$$f(t+\Delta t) \approx f(t) + \Delta t f'(t) + \frac{(\Delta t)^2}{2!} f''(t) + \dots + \frac{(\Delta t)^n}{n!} f^{(n)}(t), \tag{29}$$

the remainder is given by

$$(\text{remainder}) = \frac{(\Delta t)^{n+1}}{(n+1)!} f^{(n+1)}(\tau), \quad t \leqslant \tau \leqslant t + \Delta t. \tag{30}$$

The time increment Δt is calculated so that the remainder (30) should be equal to some small error limit ε. For a given value of ε, Δt is determined by

$$\Delta t = \left(\frac{\varepsilon (n+1)!}{f^{(n+1)}(\tau)} \right)^{1/(n+1)}. \tag{31}$$

$f^{(n+1)}(\tau)$ is approximated as

$$f^{(n+1)}(\tau) \approx \max_{1 \leqslant i \leqslant N} \left\{ \left| \left(\frac{D^{n+1}\xi}{Dt^{n+1}} \right)_i \right|, \left| \left(\frac{D^{n+1}\eta}{Dt^{n+1}} \right)_i \right|, \left| \left(\frac{D^{n+1}\phi}{Dt^{n+1}} \right)_i \right| \right\}, \tag{32}$$

where N is the total number of nodes on the free surface. The Lagrangian time derivatives up to the nth order are computed by the procedure explained previously. Then the $(n+1)$th-order Lagrangian derivatives are evaluated using appropriate backward finite difference schemes with the nth-order derivatives. Only at the first time step, namely at $t = 0$, are the $(n+1)$th-order Lagrangian derivatives in (32) replaced by the nth-order Lagrangian derivatives, because no backward finite difference schemes are available at $t = 0$. From such an approximation, it follows that Taylor series truncated at the term of $(n-1)$th-order derivatives are used to calculate the values of ξ, η and ϕ at $t = \Delta t$.

CHECKS OF COMPUTATIONAL ACCURACY

Figure 1 shows a simplified model of the experimental equipment used by Hammack.[8] By comparing the numerical results with the experimental data obtained by Hammack, the computational accuracy of the present method is examined.

Computations are carried out for three piston motions with different ascending velocities: impulsive motion, transitional motion and creeping motion.

The size of the water tank and the values of the parameters for the computations are summarized in Table I. All the quantities used in the present computations are non-dimensionalized with the acceleration due to gravity, g, and the uniform depth of water, h. In the impulsive and transitional motions, a finer element discretization has been done along the centreline of the tank than in the creeping motion.

Figures 4–6 show the time histories of the free surface displacement at the station $x/h = 0$. The present numerical results are denoted by open circles and the experimental data are denoted by solid lines. The computed results by the linear theory of Hammack are also shown by broken lines. Agreement between the computed and experimental values is good, and the difference

Table I. Parameters for computations

Motion	W/h	b/h	Number of elements Γ_1	Γ_2	Γ_3	ε	Y_0/h	$\alpha\sqrt{(h/g)}$
Impulsive	40·0	12·2	100	20	61	10^{-5}	0·2	1·305
Transitional	40·0	12·2	100	20	61	10^{-5}	0·1	0·231
Creeping	100·0	12·2	100	10	37	10^{-5}	0·3	0·010

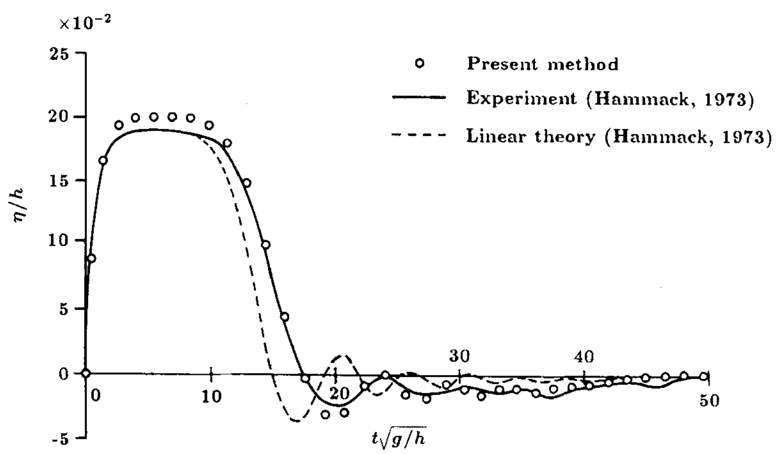

Figure 4. Time histories of the free surface displacement at the station $x/h = 0$ in the impulsive motion of the piston

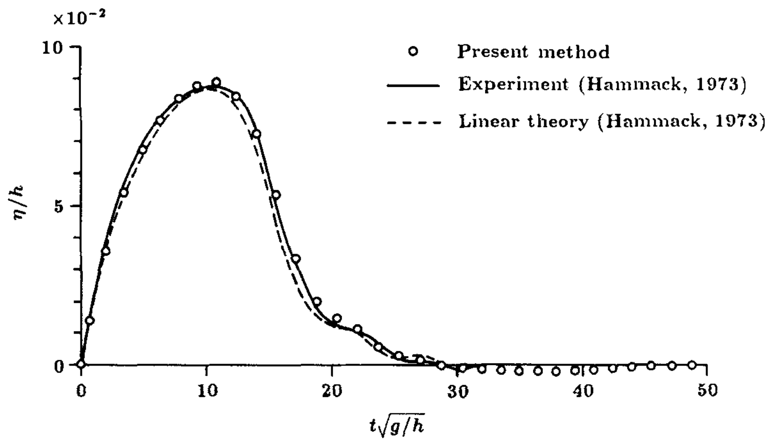

Figure 5. Time histories of the free surface displacement at the station $x/h = 0$ in the transitional motion of the piston

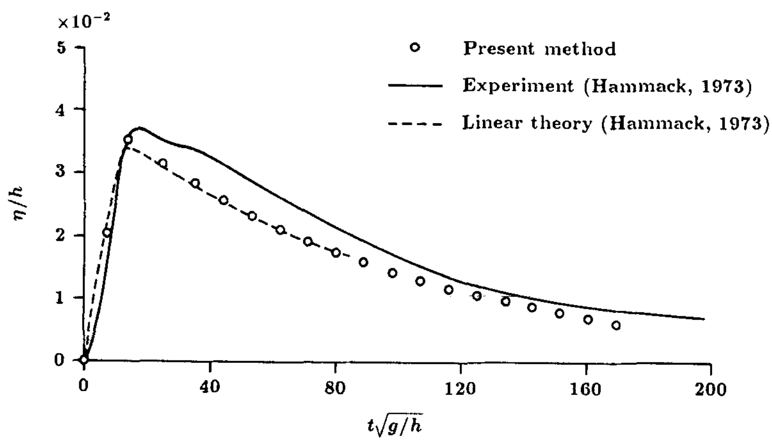

Figure 6. Time histories of the free surface displacement at the station $x/h = 0$ in the creeping motion of the piston

between the present numerical results and those of the linear theory is clear. In Figure 6 the plotting of the numerical results has been terminated at $t\sqrt{(g/h)} = 169.6$, because the influence of a reflecting wave from the right wall of the tank has appeared at the station $x/h = 0$.

Another check of accuracy has been done by calculating, at each time step,

$$Q = \int_{\Gamma} \frac{\partial \phi}{\partial n} \, d\Gamma \tag{33}$$

and

$$H = \int_{\Gamma_1} \eta \, dx - bY_P(t). \tag{34}$$

The quantity Q represents the total outflow across the boundary $\Gamma(=\Gamma_1+\Gamma_2+\Gamma_3)$. By applying Gaussian divergence theorem to equation (33), it is found that Q is expressed as

$$Q=\int\int_{\Omega}\nabla^2\phi\,\mathrm{d}x\mathrm{d}y \tag{35}$$

and that Q should vanish. The quantity H is related to the conservation of the mass of fluid and should apparently vanish. The numerical values of Q and H have been obtained by changing equations (33) and (34) into

$$Q=\int_{\Gamma}\frac{\partial\phi}{\partial n}\frac{\mathrm{d}s}{\mathrm{d}\zeta}\mathrm{d}\zeta, \tag{36}$$

$$H=\int_{\Gamma_1}\eta\frac{\mathrm{d}x}{\mathrm{d}\zeta}\mathrm{d}\zeta-bY_{\mathrm{P}}(t) \tag{37}$$

and integrating them by the trapezoidal rule. Here ζ is a supplementary variable as given in the Appendix.

The non-dimensional forms of Q and H are defined as

$$Q^*=\frac{Q}{\sqrt{(gh^3)}},\qquad H^*=\frac{H}{h^2},$$

where an asterisk denotes a non-dimensional quantity. The maximum and minimum values of $|Q^*|$ and $|H^*|$ are tabulated in Table II. In the creeping motion, these values were computed in the interval between $t\sqrt{(g/h)}=0$ and $t\sqrt{(g/h)}=169{\cdot}6$ for the reason mentioned above.

In Table III the size of the time increment is listed. Although the reduction of ε results in smaller size of time increment, it has little influence on the values of Q and H. To reduce Q and H, finer discretizations of the boundary may be needed.

All the computations have been carried out on a minicomputer, Celerity C-1260, which is comparable to the VAX 8600. The CPU time is about 90 min per 100 time steps in the case of the transitional motion. The case of the transitional motion has also been analysed in Reference 6. Comparing the present method with that of Reference 6, the former requires only one-third of the computing time of the latter. The use of the variable time-stepping method makes a great contribution to the increase in the computing speed of the present method.

Table II. Checks of computational accuracy

Motion	$\lvert Q^*\rvert_{\max}$	$\lvert Q^*\rvert_{\min}$	$\lvert H^*\rvert_{\max}$	$\lvert H^*\rvert_{\min}$
Impulsive	$1{\cdot}4\times10^{-4}$	$8{\cdot}3\times10^{-7}$	$5{\cdot}6\times10^{-3}$	$9{\cdot}2\times10^{-6}$
Transitional	$4{\cdot}6\times10^{-5}$	$3{\cdot}6\times10^{-7}$	$1{\cdot}0\times10^{-3}$	$2{\cdot}8\times10^{-6}$
Creeping	$8{\cdot}0\times10^{-5}$	$1{\cdot}9\times10^{-9}$	$6{\cdot}8\times10^{-4}$	$3{\cdot}1\times10^{-6}$

Table III. Size of the time increment ($\varepsilon=10^{-5}$)

Motion	$[\Delta t\sqrt{(g/h)}]_{\max}$	$[\Delta t\sqrt{(g/h)}]_{\min}$	$[\Delta t\sqrt{(g/h)}]_{\mathrm{average}}$
Impulsive	0·338	0·047	0·294
Transitional	0·564	0·178	0·508
Creeping	1·035	0·373	0·871

CONCLUDING REMARKS

A numerical method has been developed for the analysis of unsteady free surface flow problems which are formulated mathematically on the basis of the potential flow theory. The algorithm is very simple. Throughout the computations it has been found that the combined use of a Taylor series expansion in time with a variable time-stepping technique makes the present method accurate and numerically stable. These facts encourage us to extend the present method for the analysis of three-dimensional problems.

ACKNOWLEDGEMENTS

The author would like to express his sincere gratitude to Professor Masaru Mizuguchi (Chuo University) for his valuable advice, including some information about the original method of Dold *et al.* The author also wishes to express his sincere thanks to the referees for their valuable comments.

This work has been supported by the Japanese Ministry of Education, Science and Culture under Grant-in-Aid for Scientific Research.

APPENDIX: NUMERICAL DIFFERENTIATION

The derivations of the formulae used in the numerical differentiation are briefly described.[1,9]

Since the nodal points on the free surface are moved every time step in a Lagrangian manner, they are not necessarily spaced equally along the free surface. Thus it will be convenient to map the free surface onto an auxiliary axis on which the nodal points are spaced equally. Let ζ denote the nodal number along the free surface and consider ζ as a continuous real variable. Then it follows that the nodal points on the free surface are spaced equally along the ζ-axis (Figure 7). Since x, y, u and v can be considered as functions of ζ on the ζ-axis, the relations

$$\frac{\partial u}{\partial \zeta} = \frac{\partial u}{\partial x}\frac{\mathrm{d}x}{\mathrm{d}\zeta} + \frac{\partial u}{\partial y}\frac{\mathrm{d}y}{\mathrm{d}\zeta}, \tag{38}$$

$$\frac{\partial v}{\partial \zeta} = \frac{\partial v}{\partial x}\frac{\mathrm{d}x}{\mathrm{d}\zeta} + \frac{\partial v}{\partial y}\frac{\mathrm{d}y}{\mathrm{d}\zeta} \tag{39}$$

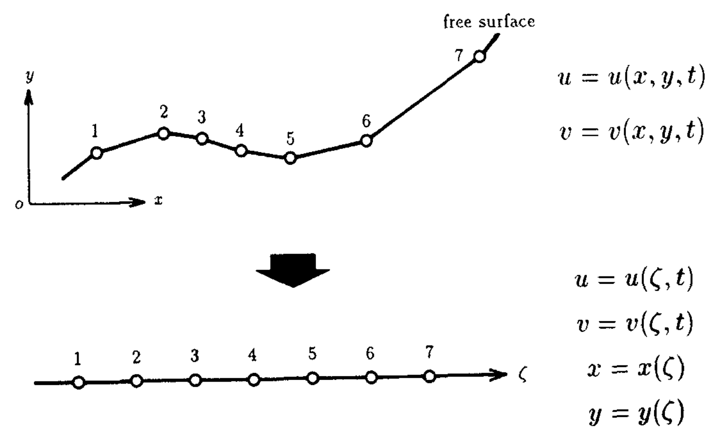

Figure 7. Mapping of the free surface onto the ζ-axis

exist. Applying the equation of continuity

$$\frac{\partial u}{\partial x} + \frac{\partial v}{\partial y} = 0 \tag{40}$$

and the irrotational condition

$$\frac{\partial v}{\partial x} - \frac{\partial u}{\partial y} = 0 \tag{41}$$

to equations (38) and (39) yields

$$\frac{\partial u}{\partial \zeta} = \frac{\partial u}{\partial x}\frac{\mathrm{d}x}{\mathrm{d}\zeta} + \frac{\partial v}{\partial x}\frac{\mathrm{d}y}{\mathrm{d}\zeta}, \tag{42}$$

$$\frac{\partial v}{\partial \zeta} = \frac{\partial v}{\partial x}\frac{\mathrm{d}x}{\mathrm{d}\zeta} - \frac{\partial u}{\partial x}\frac{\mathrm{d}y}{\mathrm{d}\zeta}. \tag{43}$$

The solution of this set of equations for $\partial u/\partial x$ and $\partial v/\partial x$ gives

$$\frac{\partial u}{\partial x} = \frac{1}{D}\left(\frac{\partial u}{\partial \zeta}\frac{\mathrm{d}x}{\mathrm{d}\zeta} - \frac{\partial v}{\partial \zeta}\frac{\mathrm{d}y}{\mathrm{d}\zeta}\right), \tag{44}$$

$$\frac{\partial v}{\partial x} = \frac{1}{D}\left(\frac{\partial u}{\partial \zeta}\frac{\mathrm{d}y}{\mathrm{d}\zeta} + \frac{\partial v}{\partial \zeta}\frac{\mathrm{d}x}{\mathrm{d}\zeta}\right), \tag{45}$$

where

$$D = \left(\frac{\mathrm{d}x}{\mathrm{d}\zeta}\right)^2 + \left(\frac{\mathrm{d}y}{\mathrm{d}\zeta}\right)^2. \tag{46}$$

Then, if the derivatives of x, y, u and v with respect to ζ can be computed, we can evaluate $\partial u/\partial x$ and $\partial v/\partial x$. Once $\partial u/\partial x$ and $\partial v/\partial x$ are computed, $\partial u/\partial y$ and $\partial v/\partial y$ are given using the relations (40) and (41).

The differentiation along the ζ-axis is implemented approximately by appropriate finite difference schemes. In the present method the following central difference formula is used:[10]

$$f'(\zeta_0) \approx \frac{f_{-2} - 8f_{-1} + 8f_1 - f_2}{12h}, \tag{47}$$

where

$$f_{\pm k} = f(\zeta_0 \pm kh) \quad (k = 1, 2). \tag{48}$$

Here h represents the interval between two neighbouring nodes on the ζ-axis and is equal to unity. At both ends of the free surface the backward difference formula

$$f'(\zeta_0) \approx \frac{25f_0 - 48f_{-1} + 36f_{-2} - 16f_{-3} + 3f_{-4}}{12h}, \tag{49}$$

$$f_{-k} = f(\zeta_0 - kh) \quad (k = 1, 2, 3, 4), \tag{50}$$

and the forward difference formula

$$f'(\zeta_0) \approx \frac{-25f_0 + 48f_1 - 36f_2 + 16f_3 - 3f_4}{12h}, \tag{51}$$

$$f_k = f(\zeta_0 + kh) \quad (k = 1, 2, 3, 4), \tag{52}$$

are used.

Next the tangential derivative of ϕ can be calculated in a similar way. It is expressed as[1]

$$\frac{\partial \phi}{\partial s} = \left(\frac{\partial \phi}{\partial \zeta}\right) \Big/ \left(\frac{\mathrm{d}s}{\mathrm{d}\zeta}\right), \tag{53}$$

and $\mathrm{d}s/\mathrm{d}\zeta$ is written as

$$\frac{\mathrm{d}s}{\mathrm{d}\zeta} = \sqrt{\left[\left(\frac{\mathrm{d}x}{\mathrm{d}\zeta}\right)^2 + \left(\frac{\mathrm{d}y}{\mathrm{d}\zeta}\right)^2\right]}. \tag{54}$$

Thus $\partial\phi/\partial s$ can be evaluated by differentiating x, y and ϕ with respect to ζ by the finite difference schemes mentioned above.

REFERENCES

1. M. S. Longuet-Higgins and E. D. Cokelet, 'The deformation of steep surface waves on water: I. A numerical method of computation', *Proc. R. Soc. Lond. A*, **350**, 1–26 (1976).
2. T. Vinje and P. Brevig, 'Numerical simulation of breaking waves', *Adv. Water Resources*, **4**, 77–82 (1981).
3. O. M. Faltinsen, 'A numerical nonlinear method of sloshing in tanks with two-dimensional flow', *J. Ship Res.*, **22**, 193–202 (1978).
4. T. Nakayama and K. Washizu, 'The boundary element method applied to the analysis of two-dimensional nonlinear sloshing problems', *Int. j. numer. methods eng.*, **17**, 1631–1646 (1981).
5. P. L.-F. Liu and J. A. Liggett, 'Application of boundary element methods to problems of water waves', in P. K. Banerjee and R. P. Shaw (eds), *Developments in Boundary Element Methods—2*, Applied Science Publishers, London, 1982, pp. 37–67.
6. T. Nakayama, 'Boundary element analysis of nonlinear water wave problems', *Int. j. numer. methods eng.*, **19**, 953–970 (1983).
7. J. W. Dold and D. H. Peregrine, 'Steep unsteady water waves: an efficient computational scheme', *Proc. Nineteenth Coastal Engineering Conf.*, Houston, TX, 1984, pp. 955–967.
8. J. L. Hammack, 'A note on tsunamis: their generation and propagation in an ocean of uniform depth', *J. Fluid Mech.*, **60**, Part 4, 769–799 (1973).
9. M. Mizuguchi, Private communications (1988).
10. C. F. Gerald and P. O. Wheatley, *Applied Numerical Analysis*, 3rd edn, Addison-Wesley, Menlo Park, CA, 1984.